HE 2.1.4

THE ELECTRON/MUON RATIO IN EAS AT AND ABOVE THE "KNEE" REGION

J. H. Weber[1] for the KASCADE Collaboration[2]

[1] *Forschungszentrum Karlsruhe, Institut für Kernphysik, D 76021 Karlsruhe, Germany*

ABSTRACT

New data on the electron/muon ratio measured by the KASCADE extensive air shower experiment are presented. This ratio has been proven to be an important parameter for the determination of the mass of the primary particle. The electron and muon detector responses and reconstruction accuracies of the shower parameters have been studied in detailed simulations. Due to the extended lateral distribution of the muons at ground level, reconstruction of the total muon number is affected by the limited area of the experiment (200×200 m^2). Reconstructed and simulated muon density distributions are, therefore, restricted to the geometrical acceptance range of the experiment and are compared only within this region. Measuring the ratio as a function of the muon number, we observe a trend towards a heavier composition with increasing energy.

EXPERIMENTAL SETUP AND OBSERVABLES

The KASCADE detector array measures the lateral electron and muon distributions of extensive air showers. One aim is to obtain the electron and muon numbers that give important hints to the mass and energy of the primary particle. The array comprises about 500 m^2 of e/γ- and 620 m^2 of muon detectors which are distributed over 252 detector stations and are arranged on a grid of 200×200 m^2 size. They are described in more detail elsewhere (Klages et al.,1997a, 1997b). The muon detectors are positioned directly below the e/γ detectors and are shielded by slabs of lead and iron corresponding to 20 radiation length in total. This imposes an energy threshold of 300 MeV to muons. Because of the geometrical arrangement many muons will deposit energy in the e/γ detector before entering the muon detector. On the other hand, energetic photons or electrons may penetrate the shielding, thereby faking a muon signal. To correct for these effects, the observed energy depositions produced by the different particle species were simulated for both types of detectors. The simulated air shower events were produced with the CORSIKA event generator (V. 4.6) (Capdevielle, 1992) and all particles at observation level were fully tracked through the KASCADE experiment. Since the particles and their energies on top of a detector station are known in the simulations, comparison to their average simulated energy deposition in both detectors can be used to correct the experimental data. Such a simulation has to take into account possible differences originating from different masses of the primary particle, different zenith angles etc.. Figure 1 shows as an example the expected energy deposition in the e/γ and muon detectors as a function of the distance from the shower core for proton induced showers of $E = 10^{15}$ eV, and $\theta = 22°$. As expected, the very abundant photons and electrons in the air shower deposit a large amount of energy in the e/γ detector, while hadrons and muons contribute only a very small background close to the shower core. However, at distances far from the shower core the energy deposit caused by muons becomes similar to that of electrons and photons due to their flat lateral distribution. In the muon detectors, the signal is dominated by the muons only at radii larger than 30 m.

[1]corresponding author: e-mail: weber@ik1.fzk.de

[2]A full list of authors and institutions of the KASCADE Collaboration is given at the end of this volume.

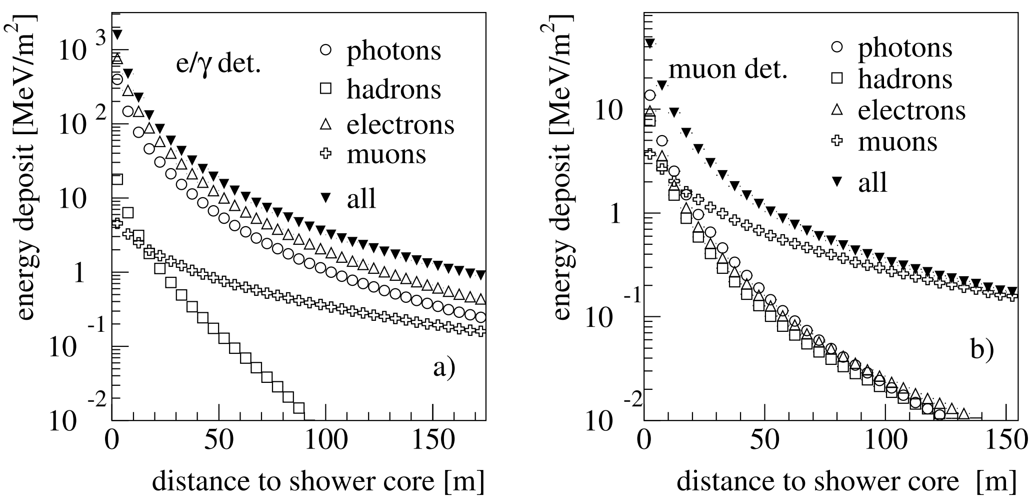

Fig. 1: Simulated energy deposit per m^2 in e/γ (a) and muon detectors (b) as a function of the distance to the shower core for proton induced showers of E=10^{15} eV and $\theta = 22°$

Close to the shower core, on the other hand, the signal is dominated by the energy deposit of hadrons and the electromagnetic punch through.

THE LATERAL ENERGY CORRECTION FUNCTION (LECF)

To correct for the experimental effects of particle detection discussed above, a large set of simulated data was produced. The simulation allows to examine the detector response for each type of particle and takes into account also their relative abundances, energy, and density distributions as a function of the distance from the shower core. With this information the following lateral energy correction functions (LECF) were calculated for proton and iron induced showers of different energies and angles: The sum of hadron, photon, and electron deposits in the e/γ detector normalized to the number of electrons (a), the muon deposit per muon in the e/γ detector (b), the sum of photon and electron deposits ('punch through') per electron in the muon detector (c), the hadron deposit per electron in the muon detector (d), and the muon deposit per muon in the muon detector (e). All these numbers were found to show only a small dependence ($\sim 5\%$) on the energy and angle (after corrections with $\cos\theta$) of the primary particle, hence averaged functions could be used. The result is shown in Figure 2.
There is a steep rise of energy deposit per electron near the shower core because of pair production processes of high energy photons. The rise with increasing distance is due to the increasing photon/electron ratio (a). Muons show a constant mean energy deposit of 9.2 MeV in the e/γ detector (b). In the muon detectors, the electromagnetic punch through (c) and the hadrons

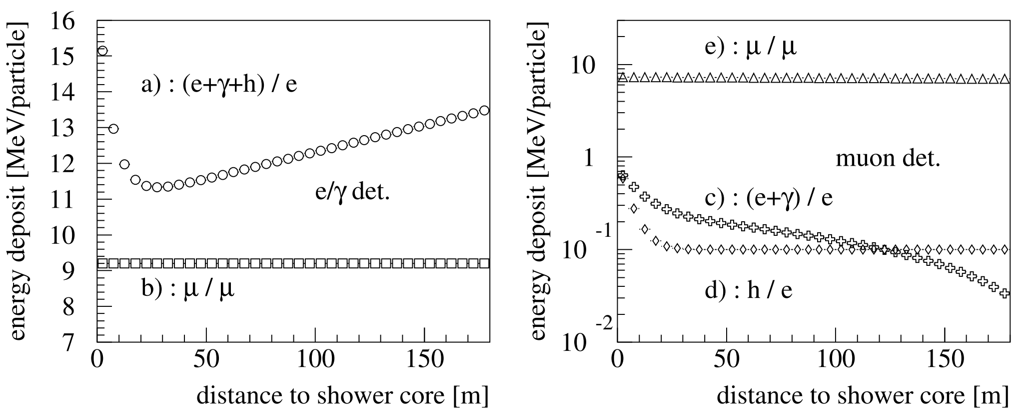

Fig. 2: Energy deposit per particle as a function of the distance to the shower core

(d) contribute mainly close to the shower core, but are of little importance at larger distances. Therefore, only muon signals outside 40 m from the shower axis are evaluated in the analyses. The hadronic energy deposit is very low on average, but individual protons or neutrons occasionally produce relatively high signals which can be recognized and flagged by the reconstruction software. Therefore an explicit correction for hadron deposits in the muon detector is not required. The higher mean muon energy near the shower core leads to the production of more secondary particles in the absorber. Hence, function (e) decreases slightly with increasing distances. The electron and muon densities in the experimental data are finally obtained by dividing the observed energy deposits in the two detectors by the corresponding lateral correction functions (LECF) a) and e), respectively. The muon deposit in the e/γ detector and the punch through are corrected by an iterative method, as discussed below.

DETERMINATION OF ELECTRON AND MUON NUMBERS

The correction and evaluation of data is performed in three levels. The first level uses uncorrected data for a rough and fast estimation of the shower parameters that are used as start parameters for subsequent fits. The core position is determined by a neural network (Mayer,1992) or by a center of gravity method, the shower direction is found by a gradient method, and the electron and muon numbers are obtained by parametrisations of the total energy deposits. In a second level, the uncorrected electron densities (= charged particle densities) are fitted in the radial range of 10 to 150 m using a NKG function with a Molière radius of 79 m. The lower cut is introduced to avoid problems caused by the limited dynamic range of the detectors close to the shower core, and the upper cut is introduced because of an increasing sensitivity of the LECFs to properties of the primary particle and because of uncertainties caused by low statistics far from the shower core. The fitted function (with an over-estimated electron number) provides a first estimate of the electron density in the muon detectors, so that the energy deposit in the muon detectors can be corrected by subtracting an energy of 0.1 MeV per electron (see Fig. 2). Due to the over-estimated electron number this results in too large corrections that can be recorrected by the help of the newly calculated muon numbers. The muon densities are fitted by a Greisen function using a fixed (but electron number and zenith angle dependent) slope parameter in the range of 40 to 200 m. The lower radius cut is due to the uncertainties discussed above and the upper cut reflects the limits of geometrical acceptance. Using this function, the energy deposits in the e/γ detectors are corrected for their muon contribution in a third level and the subsequent NKG fit provides the final electron numbers. This fitted function is, in a final step, used to correct the energy deposits in the muon detector. The muon densities are then fitted by a Greisen function again. By integrating this function from zero to infinity, we obtain the muon size, N_μ. Alternatively, an

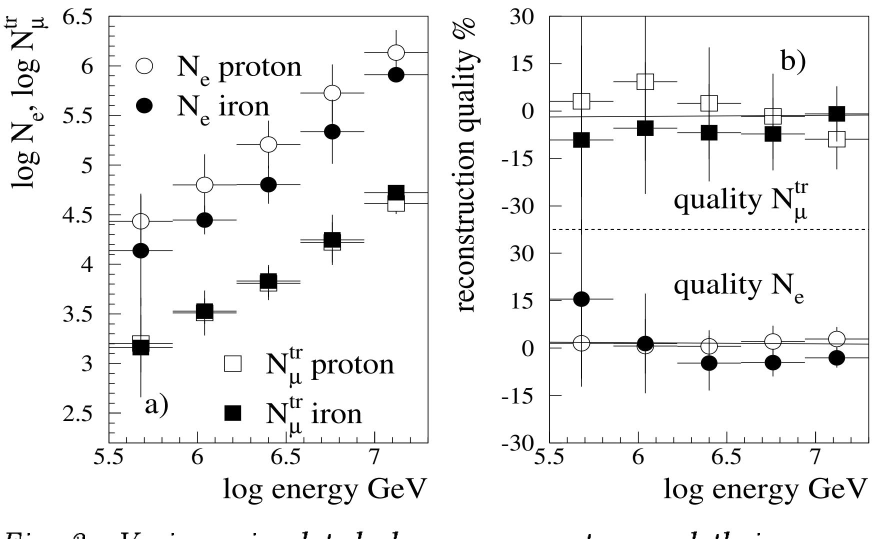

Fig. 3: Various simulated shower parameters and their reconstruction quality as function of energy. The errors bars represent the standard deviation

integration limited to the range of the fits, gives the truncated muon size, $N_\mu^{\rm tr}$, which is approximately a factor of 3 smaller than the total muon size. This observable has the advantage to be free of systematic uncertainties caused by extrapolations outside the experimental acceptance. Figure 3 a) shows the energy dependence of N_e and $N_\mu^{\rm tr}$. The truncated muon number can be considered a good energy estimator, as it shows only marginal sensitivity to the mass of the primary particle. The reconstruction quality (% deviation) of the shower parameters is shown as a function of energy in Figure 3 b). Systematical differences in the determination of the total muon numbers between proton and iron induced showers due to the fixed slope parameter in the Greisen functions are reduced by using truncated muon numbers.

THE ELECTRON/MUON RATIO

The data presented here were taken between October 1996 and March 1997. The following principal cuts were applied to the reconstructed events in order to ensure reliable reconstruction results: the reconstructed shower core lies within a radius of 91 m to the center of the array and cuts in the reconstructed electron and muon number reflect an energy threshold of approximately $5 \cdot 10^{14}$ eV. The data were subdivided into narrow zenith angles bins. To be comparable with simulations the zenith angle of the data shown in Figure 4 was restricted to $18° \leq \theta \leq 26°$. About 330,000 events survived these cuts. Figure 4 a) shows the electron number as a function of the truncated muon size for these showers. Simulated results for proton and iron induced showers are shown for comparison. These results include the detector response and the full reconstruction. Statistical errors are smaller than the size of the symbols. The simulations show the very good ability to distinguish between heavy and light particles. This is even better illustrated by dividing the electron and muon numbers for each event as is shown in figure 4 b). The data approach the proton curve and show a slight trend to a heavier composition with increasing muon number. As shown by (Glasstetter et al.,1997) the electron size spectra exhibit a ”knee” in the same region. The ongoing experiment will deliver much better statistic in the next months. A careful study of systematic effects will be continued.

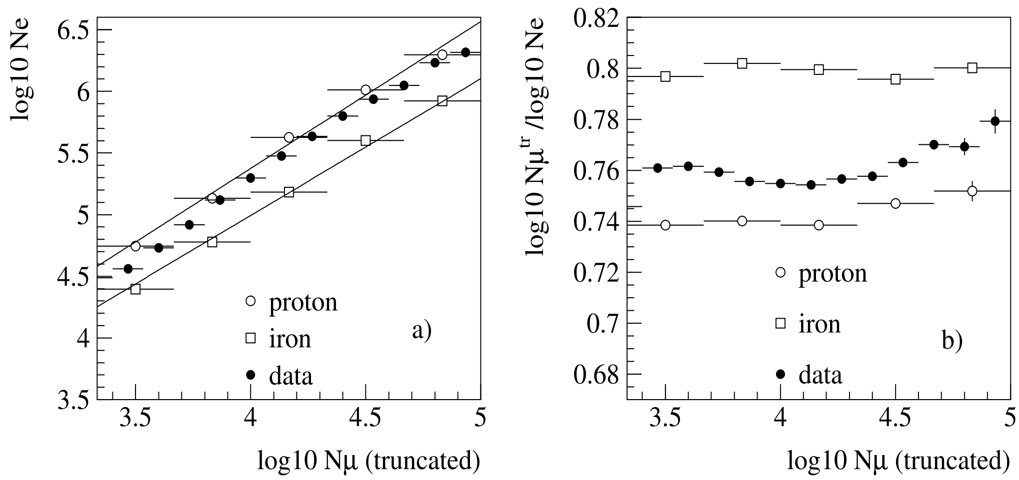

Fig. 4: Electron size (a) and muon/electron ratio (b) as a fuction of the truncated muon size

REFERENCES

Capdevielle, J.N. et al.,*Kernforschungszentrum Karlsruhe Report*, KfK 4998 (1992)

Glasstetter, R. et al., Proc.25th ICRC, Durban, HE 2.1.5 (1997)

Klages, H.O. et al., *Nucl.Phys. B (Proc.Suppl.)* 92, 52 B, (1997a)

Klages, H.O. et al., Proc. 25th ICRC, Durban, HE 2.1.1 (1997b)

Mayer,H.J., *Nucl.Instr. and Meth.* A317, 339 (1992)